

Research article

# Development of EVA/POE/SEBS microcellular foam: Network structure, mechanics performance and midsole application

Zhen Yu<sup>ID</sup>, Leyuan Ma<sup>ID</sup>, Bojiang Zhu, Ajit Dattatray Phule, Shibao Wen, Yongxian Zhao, Zhenxiu Zhang\*

Key Laboratory of Rubber–Plastics, Ministry of Education/Shandong Provincial Key Laboratory of Rubber–Plastics, Qingdao University of Science and Technology, 266042 Qingdao, China

Received 20 May 2022; accepted in revised form 9 August 2022

**Abstract.** Thermoplastic elastomer foam is often used as a midsole, which is an important factor affecting sports efficiency. In this research, ethylene vinyl acetate copolymer/polyolefin elastomer/styrene ethylene butylene styrene (EVA/POE/SEBS) microcellular foam was prepared with supercritical nitrogen gas (SC-N<sub>2</sub>). The influence of the formulation ratio on the matrix network structure was studied by vulcanization curve and rheometric expansion system rheometer. Then the foaming behavior and static/dynamic mechanical properties were studied, and midsole was prepared. The results showed that the increase of the relative content of SEBS reduced the viscosity of the matrix, but the loss factor increased, which further reduced the resistance to cell growth and increased the expansion ratio (density decreased from 0.19 to 0.13 g/cm<sup>3</sup>). In addition, the increase of SEBS resulted in an increase in the static compressive strength and resilience (61%) of the foam. However, after 100 000 dynamic compression cycles, the increase of SEBS resulted in a decrease in the energy absorption capacity of the foam and an increase in the dynamic compression set (from 6.8 to 9.4%). This is significantly different from the traditional physical and mechanical performance test results, which are rarely reported and have significance for practical applications.

**Keywords:** polymer blends and alloys, processing technologies, industrial applications, supercritical nitrogen foaming, dynamic compression

## 1. Introduction

The importance of lightweight foam material has been extensively raised, which has been applied to various industries, such as construction, packaging, aerospace, etc., also play an important role in our daily life [1–4]. For example, the midsole of sports shoes is usually made of thermoplastic elastomer (TPEs) foam [5]. However, the traditional foaming method often uses organic foaming agent [6–8], resulting in environmental pollution and chemical residues. In 2010, Belgium and France announced they would remove puzzle pads from shelves, because

of excessive levels of formamide, which is classified as reprotoxic (toxic to reproduction).

Supercritical foaming was first proposed by Massachusetts Institute of Technology (MIT) in the 1980s as an eco-friendly and controllable foaming technology. The prepared foam has small cell size, large cell density and high specific strength. By controlling the process parameters such as temperature, pressure and time, high-performance foams with uniform cell size and regular cell morphology can be obtained [9, 10]. Some researchers have shown that the different polymer foams can be

\*Corresponding author, e-mail: [zhangzhenxiu@qust.edu.cn](mailto:zhangzhenxiu@qust.edu.cn)  
© BME-PT

achieved by methods such as batch foaming, injection molding and extrusion techniques [11, 12].

Supercritical carbon dioxide (SC-CO<sub>2</sub>) and supercritical nitrogen (SC-N<sub>2</sub>) are widely applied in microcellular foaming, they have distinct physical properties, which lead to significant differences in the process as well as the product quality [13]. The critical point of CO<sub>2</sub> is 304.2 K and 7.38 MPa, and critical point of N<sub>2</sub> is 126.2 K and 3.39 MPa. Large amounts of CO<sub>2</sub> can be dissolved more readily and yield a much more profound plasticization effect on the polymer melt compared to N<sub>2</sub>, which not only achieves higher expansion rate, but also leads to the problem of size shrinkage of foaming samples [14, 15]. Researchers have successfully used supercritical nitrogen (SC-N<sub>2</sub>) to prepare foam with stable size [16]. Our research group compared the effects of SC-CO<sub>2</sub> and SC-N<sub>2</sub> on expanded thermoplastic polyurethane (ETPU) foam, and found that SC-CO<sub>2</sub> could obtain a relatively higher foaming ratio, while the SC-N<sub>2</sub> foaming ratio was relatively lower and dimensional shrinkage was relatively small [17].

Compared to other TPEs, ethylene-vinyl acetate copolymer (EVA) has a much lower cost, and is also recyclable [18]. As an ethylene-vinyl acetate copolymer, EVA has a long branch chain and is easy to form a crosslinking structure, which provides sufficient melt strength for supercritical foaming [19, 20]. In addition, the CH<sub>3</sub>COO side reduces the regularity of macromolecules and provides EVA molecular chains with better elasticity and lower hardness [21]. In addition, compared to EVA foam, the blend foam of EVA with other polymers tends to have better plasticity, elasticity, wear resistance and lightweight than pure EVA [22, 23]. Zhang *et al.* [24] prepared EVA/polyurethane (EVA/PU) blends foam by SC-N<sub>2</sub>, the results showed that EVA/PU foam had higher hardness, toughness, friction coefficient and wear resistance than EVA foam, but lower compression consolidation, tensile strength and tear strength. However, as a shoe midsole material, the cushioning performance is quite important, but increasing the cushioning performance often comes at the expense of reducing elasticity, and vice versa.

Poly(styrene-*b*-(ethylene-*co*-butylene)-*b*-styrene) (SEBS) are widely applied TPEs with a hard end-block polystyrene phase and a soft elastomeric phase, which has high resilience [25–27]. Yamaguchi *et al.*

[28] reported that the friction coefficient of the EVA foam increased with porosity when slid against a smooth surface, whereas its friction coefficient increased with porosity and SEBS fraction when slid against a rough surface. Polyolefin thermoplastic elastomers (POE) are random ethylene-octene copolymers with relatively low melting temperatures ( $T_m$ ) and elastic recovery that is tunable and dependent on comonomer content [29]. SEBS and polyolefin elastomer (POE) are often mixed with polyolefins to improve their supercritical foaming performance, such as SEBS/PP, SEBS/PS and PP/POE foam prepared with physical foaming with SC-CO<sub>2</sub> which showed improved rheological and mechanical properties [30, 31]. However, there are few reports on the application of supercritical foaming multiphase blend foam for midsole application, especially the effect of the components on the dynamic compression behavior of foam [32].

In this research, EVA/POE/SEBS blend foam was prepared by SC-N<sub>2</sub>, and midsole was prepared by pilot-scale test. By changing the relative content of SEBS, the rheological behavior, foaming properties and static/dynamic mechanical properties of the foam-blends were studied, and the influence mechanism of the matrix network structure on the physical-mechanical properties of the foams was described. More importantly, 100 000 times of reciprocating compression experiments were used to simulate the force scenario of midsole in reality. This innovative processing technology and testing scheme provides a new idea and experimental basis for the research and application of midsole.

## 2. Materials and methods

### 2.1. Materials

The EVA with vinyl acetate content of 26% was obtained from Formosa Plastic Corporation (7470M, Taibei, China); POE was supplied by Dow Chemical Company (8150, Midlands, USA); SEBS copolymers with styrene/ethylene-butylene ratio of 20/80 was purchased from Asahi Kasei Corporation (Tuftec™ P1083, Tokyo, Japan); bis(*tert*-butyldioxyisopropyl) benzene (BIPB) as a peroxide crosslinking agent was purchased from Akzo Nobel Co. (≥98%, Amsterdam, Netherlands); xylene was purchased from Macklin Inc. (99%, Shanghai, China); N<sub>2</sub> was purchased from Qingdao Yonglaikang Gas Co., Ltd. (≥99.5%, Qingdao, China).

## 2.2. Preparation of EVA/POE/SEBS foam with SC-N<sub>2</sub> foaming method

EVA with 60 phr was added into the inner mixer (XSS-300, Kechuang Rubber and Plastic Machinery Equipment Co., Ltd., Shanghai, China), which has been heated to 130 °C firstly. After the torque image ran smoothly for 2 min, POE and SEBS were added into the inner mixer (The formula is shown in Table 1). After the torque image ran smoothly for 2 min, 0.6 phr BIPB was added and the temperature was raised to 170 °C, then the mixer was finished after the torque image ran smoothly for 4 min. Then, the blends were transferred to a double-roll mixer (X(S)K-160B, Shuangyi Rubber & Plastic Machinery Co., Ltd., Shanghai, China) to prepare raw rubber sheet. The raw rubber sheet was compressed and molded at 10 MPa for 10 min in a plate vulcanizing machine (Dongfang Machinery Co. Ltd., Huzhou, China) to prepare vulcanized rubber sheet (200 mm × 150 mm × 8 mm), the cooled at 25 ± 5 °C.

Foaming process was carried out in a 10 l autoclave with an oil heating system and connected to N<sub>2</sub> cylinders by a pressure pump. First, the autoclave was heated to 100 °C, and the vulcanized rubber sheet was put into it. Then the autoclave was sealed and N<sub>2</sub> was pumped into it to increase the internal pressure to 20 MPa for 6 hours to achieve the saturation of SC-N<sub>2</sub> in the sheet. Finally, the outlet valve

of the autoclave was opened quickly to release the pressure and obtain foam.

## 2.3. Characterization

### 2.3.1. Rheological characterizations

In order to test the effect of SEBS content on blends rheological properties, 5~6 g raw rubber sheet was taken into a non-rotor vulcanizer (GT-M2000-A, Gotech Testing Machines Inc., Taibei, China) at 170 °C, and the time was 20 min.

A clean 120 mesh wire cage (the weight was  $m_1$ ) was chosen as a cage, a certain mass of sample was cut into pieces into the wire cage and the weight was  $m_2$ . The wire cage was then boiled in xylene for 8 h and then dried in an oven at 140 °C for 3 h. After cooling, the wire cage weight was measured as  $m_3$ . The gel content was calculated by the Equation (1):

$$\text{Gel content [\%]} = \frac{m_3 - m_1}{m_2 - m_1} \cdot 100 \quad (1)$$

Rheological properties were measured using a rheometric expansion system rheometer (ARES G2, TA Instruments, New Castle, USA) equipped with parallel plates with 25 mm diameter and 1 mm gap. A dynamic frequency sweep was performed from 0.1 to 100 rad/s at 100 °C in N<sub>2</sub> atmosphere.

### 2.3.2. The foam density and cell morphology

Density of the foams was measured using an electronic density meter (DX-120Y, Xiamen Qunlong Instrument Co., Ltd., Xiamen, China) by weighing the foam in air and water, the size of the foam sample was about 10 mm × 10 mm × 10 mm.

The morphology of the foam cells was examined via scanning electron microscopy (SEM, JSM-7500f, JEOL Ltd., Tokyo, Japan). Cryogenically fractured foam surfaces were sputter coated with a thin layer of gold and scanned at an acceleration voltage of 5 kV.

### 2.3.3. Physical and mechanical performance

The tensile properties and tear strength was carried out using a universal tester (AI-7000S, Gotech Testing Machines Inc., Taibei, China) according to the ASTM D412 and ASTM D624, respectively. The tensile test samples were 4 mm in thickness and 25 mm in width, and grip separation was 75 mm. The tear strength test samples were 7.5 mm in thickness and 15 mm in width, and the sample length was 152 mm, and the incision depth was 40 mm.

**Table 1.** The formulation of the EVA/POE/SEBS compounds.

Samples		1#	2#	3#	4#	5#
SEBS	[phr]	0	5.0	10.0	15.0	20.0
POE	[phr]	40.0	35.0	30.0	25.0	20.0
EVA	[phr]			60.0		
BIPB	[phr]			0.6		

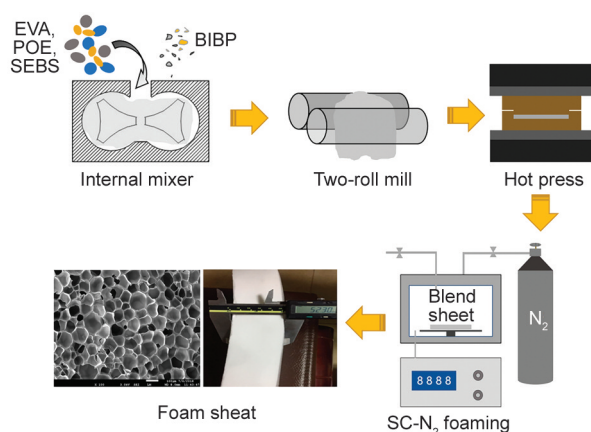


**Figure 1.** Schematic of fabrication process for EVA/POE/SEBS foam.

The hardness was performed as per ASTM D2240 using an Asker C Durometer (LX-C, Hua Rui Han Pu Detection Instrument Co., Ltd., Dongguan, China). The thickness was 10 mm, and the area was greater than 50 mm × 50 mm. The point to be measured should be at least 12 mm from the edge of the sample.

The resilience tests were performed according to ASTM D3574 standard using a ball rebound tester (Zwick 3107, Zwick Roell, Cologne, Germany). The thickness was 50 mm, and the area was 100 mm × 100 mm. The resilience value ( $R$ ) can be calculated the Equation (2):

$$R = \frac{h}{h_{\max}} \cdot 100 \quad (2)$$

where  $h$  is the ball rebound height [mm],  $h_{\max}$  is the height of the drop (500 mm).

The constant deflection compression set test was tested at a strain of 50% for 6 h at 50 °C and compression set was recorded at 30 min after releasing stress. The sample size was 50 mm × 50 mm × 25 mm.

### 2.3.4. Dynamic compression performance

To assess how durable the foam may be when integrated into footwear, the dynamic compression test was developed by using a servo hydraulic elastomer test system (MTS 831.50, MTS System Co., Ltd., Minneapolis, USA) [32]. A defined maximum 1500 N after 100 ms; zero force after 100 ms; cycle repeated after 700 ms (Figure 2). The different EVA/POE/SEBS foam samples with diameter of 50 mm and thickness of 10 mm were tested for 1000 pre-cycles, 100 000 conditioning cycles and 1000 post-cycles. A programmed force-time curve was obtained and the following results were recorded and calculated: the dynamic compression set ( $DCS$ ) = (thickness pre – thickness post)/thickness pre · 100%; the average stiffness ( $AS$ ) values between 0 N and 1500 N = force/compression; the instantaneous stiffness ( $IS$ ) =

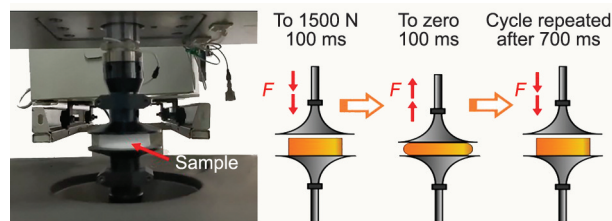


**Figure 2.** MTS testing system and schematic force-time program.

slope of force-compression curve at 645 N; energy absorbed per volume ( $EA/V$ ) = energy absorbed/the sample volume; energy efficiency ( $EE$ ) = energy returned/energy absorbed.

## 3. Results and discussion

### 3.1. Vulcanization characteristics of EVA/POE/SEBS sheet

The vulcanization characteristics of the samples with different SEBS content are shown in Table 2. The highest torque ( $M_H$ ) and the lowest torque ( $M_L$ ) were decreased with the increase of SEBS content, as did  $M_H - M_L$ . The scorch time  $t_{10}$  and the positive vulcanization time  $t_{90}$  were also gradually reduced. This attributed to the reduction in the degree of vulcanization of the blend after addition of SEBS, which could also be demonstrated by the decrease in gel content (Figure 3). As the content of SEBS increased, the number of vulcanization active sites decreased. Besides, the fracture of the small number of unsaturated double bonds contained in such SEBS might also have an effect. Therefore, the values of  $M_H$ ,  $M_L$  and  $M_H - M_L$  all showed a decreasing trend.

**Table 2.** Vulcanization parameters of EVA/POE/SEBS.

SEBS content [phr]	Scorch time, $t_{10}$ [s]	Cure time, $t_{90}$ [s]	$M_H$ [dN·m]	$M_L$ [dN·m]	$M_H - M_L$ [dN·m]
0	151	813	4.07	0.15	3.92
5	143	789	3.88	0.15	3.73
10	149	791	3.40	0.15	3.25
15	148	791	3.11	0.14	2.97
20	148	791	2.99	0.13	2.86

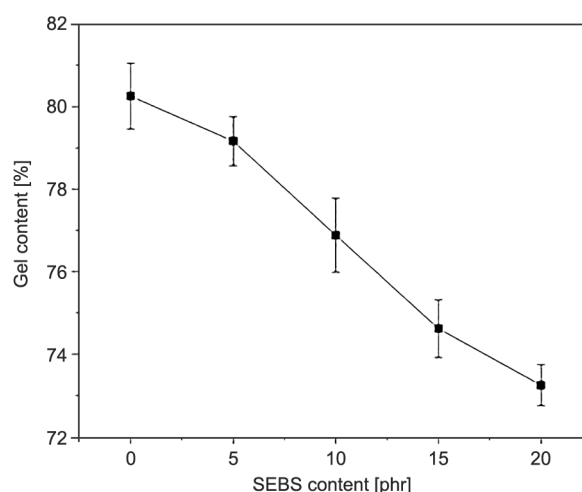


**Figure 3.** Effect of SEBS content on gel content of EVA/POE/SEBS compounds.



### 3.2. Rheological properties of EVA/POE/SEBS sheet

The viscosity influences the foaming of the material. When the viscosity is lower, the gas easily escapes from the polymerization matrix during the foaming process, which makes difficulties for nucleation to form an effective cell structure; while at the higher viscosity, the gas nucleation and cell growth are limited and then it is difficult for matrix to expand to form required final version [33]. Therefore, an appropriate viscosity is an inevitable requirement for a polymer matrix material to achieve the required version of foam. In order to further study the influence of SEBS on the sample network structure, Figure 4 shows the rheological behavior at different SEBS content with a varied frequency from 0.1 to 100 rad/s. As the SEBS increased, the complex viscosity, storage modulus and loss modulus of the blends decreased, and the  $\tan \delta$  increased. This might be because the hard segment PS in SEBS, as an incompatible phase, reduced the interaction force of the chain segment and crosslinking degree of the matrix (Figure 3), thus resulting in a decrease in viscosity. In Figure 4d, the loss factor ( $\tan \delta$ ) is the ratio of loss

modulus to storage modulus, representing the relationship between matrix viscosity and elasticity. With the increase of SEBS content,  $\tan \delta$  value increased, indicating that the influence of SEBS on the matrix storage modulus is less than the influence on the loss modulus.

### 3.3. Morphology and density of EVA/POE/SEBS foam

SEM images showed that with the increase of SEBS content, the cells size of foam showed an upward trend and the cells were more uniform (Figure 5). In the foam without SEBS, more small cells could be seen interspersed between large cells, with uneven overall structure (Figure 5a). With the increase of SEBS content, the number of small cells gradually decreased (Figure 5b–5e). This was because cell growth would be limited by the matrix network structure. The increase of crosslinking degree will enhance the density of matrix network structure, resulting in greater resistance to cell growth, thus forming small cells [34]. The addition of SEBS reduced the vulcanization degree (Figure 3 and Table 2) and viscosity (Figure 4a), thus reducing the resistance to

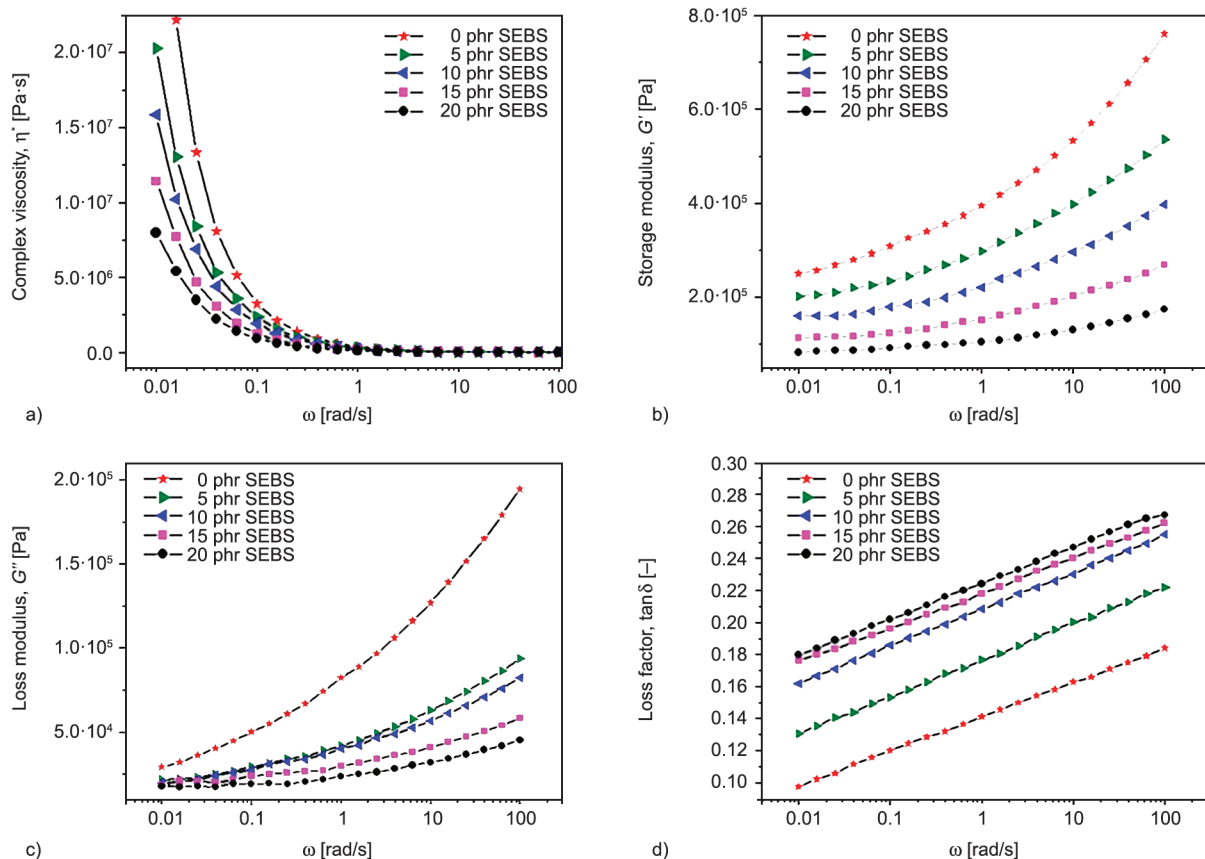


**Figure 4.** Rheological behavior of EVA/POE/SEBS sheet: a) complex viscosity,  $\eta^*$ , b) storage modulus,  $G'$ , c) loss modulus,  $G''$ , d) loss factor  $\tan \delta$ .

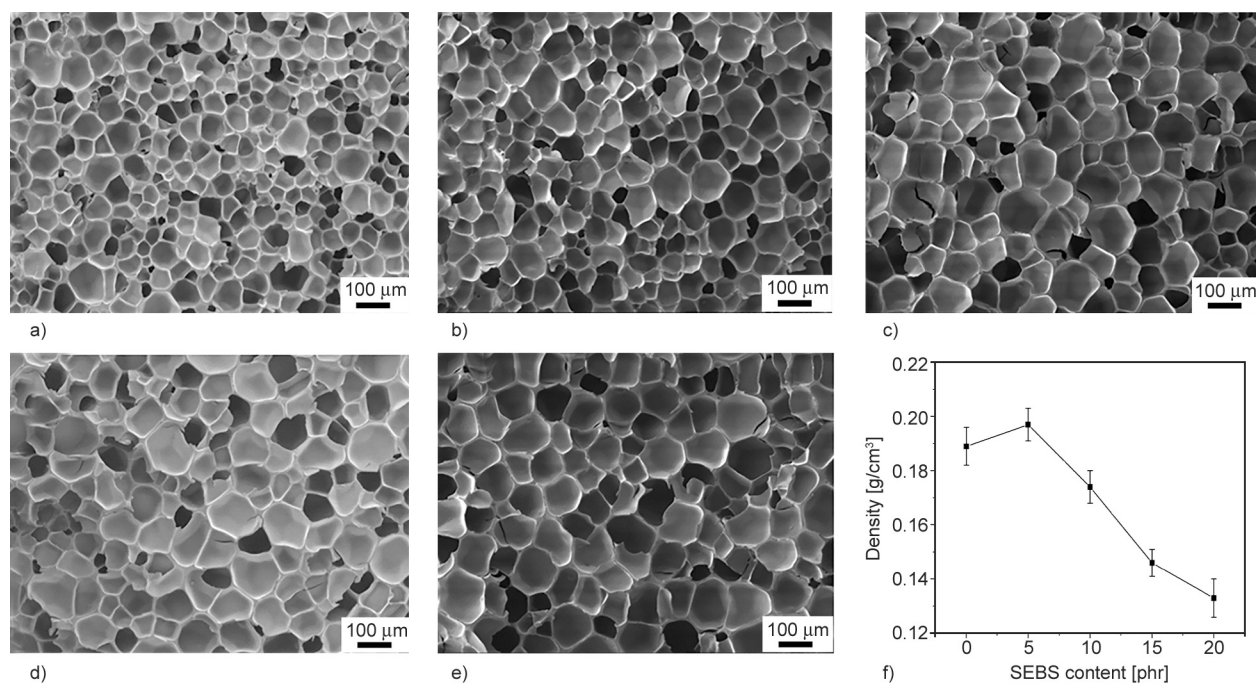


**Figure 5.** SEM images (a–e) and density (f) of the foam with varied SEBS content: a) 0 phr, b) 5 phr, c) 10 phr, d) 15 phr, e) 20 phr.

cells growth and facilitating the formation of larger cells.

In addition, the addition of SEBS made the cell size more uniform, indicating that SEBS could make the blends form more uniform network structure, which was related to the heterogeneous nucleation of hard segment polystyrene in SEBS. It was also because of heterogeneous nucleation and uniform, dense and larger cellular structure that foam density gradually decreases with the increase of SEBS content (Figure 5f).

### 3.4. Mechanical properties of EVA/POE/SEBS foam

The effects of SEBS content on the mechanical properties of the foam are shown in Figure 6. The tensile strength, tear strength and hardness decreased with the increasing of SEBS content. This was due to the fact that the overall degree of crosslinking slightly decreased with the increase of SEBS. On the other hand, the viscosity also slightly reduced ( $M_H$  was reduced from 4.07 to 2.99 [dN·m]), which also affected the mechanical properties of the foam. In addition, the increase of SEBS content effectively reduced the compression set and increased the resilience of EVA/POE/SEBS foam. When the SEBS content was 20 phr, the compression set of EVA/POE/SEBS foam decreased from 20.5 to 16.1%, and the resilience

increased from 56 to 61%, which was of great significance in the field of sports equipment.

### 3.5. Dynamic compression properties of EVA/POE/SEBS foam midsole

In order to assess durability of the midsole when integrated into footwear, the dynamic compression test was developed. The force-strain curve is shown in Figure 7, and the dynamic compression performance parameters were summarized in Table 3. As shown in Figure 7, with the increase of SEBS content, the slope of hysteresis curve before dynamic compression became smaller, while the slope of hysteresis curve after compression gradually increased, and the difference between them also increased. This was because SEBS reduced the vulcanization degree of the sample (Table 2), thus reducing the network structure stability of the sample. In addition, the  $\tan\delta$  value of the sample increased with the increase of SEBS content (Figure 4d), indicating that the proportion of the viscous part in the viscoelastic region of the sample increased, resulting in plastic deformation of the material after cyclic compression and an increase in DCS value (Table 3). It was clear that the increase in plastic deformation after reciprocating compression also led to a decrease in  $EA/V$  and  $EE$ , which was represented by an increase in sample stiffness, including  $AS$  and  $IS$ .

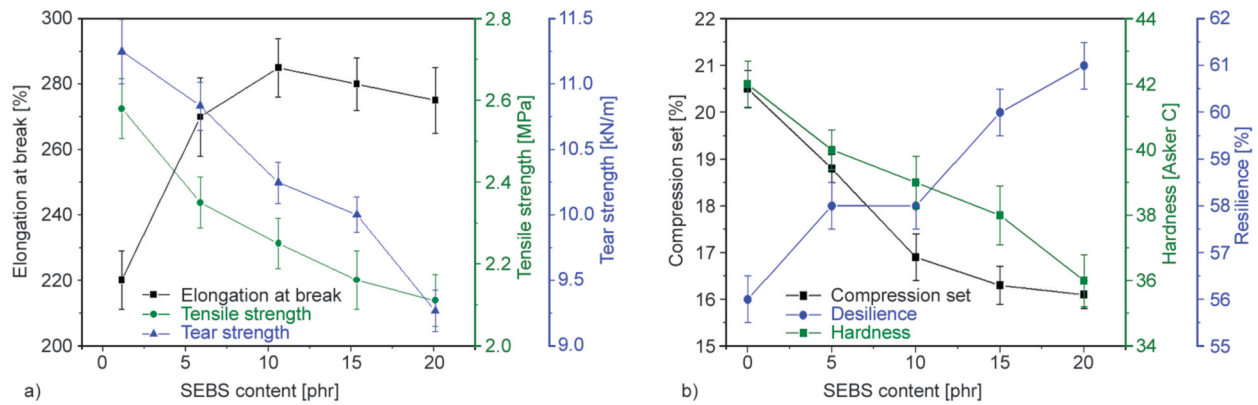


**Figure 6.** Mechanical properties of the foam with varied SEBS content: a) elongation at break, tensile strength and tear strength, b) compression set, hardness and resilience.

**Table 3.** Dynamic compression properties of the foams with different SEBS content.

SEBS content [phr]	Pre/Post	DCS [%]	EA/V [mJ/cm <sup>3</sup> ]	AS [N/mm]	IS [N/mm]	EE [–]
0	Pre	6.76	133.2	238	475	0.81
	Post		112.7	272	576	0.80
5	Pre	9.90	127.7	227	463	0.80
	Post		104.7	332	700	0.79
10	Pre	9.28	125.8	223	456	0.80
	Post		98.0	354	751	0.79
15	Pre	9.68	124.2	221	450	0.79
	Post		97.9	386	833	0.78
20	Pre	9.40	123.2	215	431	0.79
	Post		96.6	403	857	0.78

A comprehensive comparison of data before and after dynamic compression (Table 3) and data of physical and mechanical properties (Figure 6) showed that although the increase of SEBS content could increase the resilience, flexibility and energy absorption of EVA/POE/SEBS foam, the presence of SEBS would reduce the energy absorption effect and increase the plastic deformation and stiffness of the foam after 100 000 times of cyclic compression. This was a rarely reported result. Therefore,

the performance of foam should be controlled by controlling the content of SEBS, considering the specific usage scenarios of foam.

#### 4. Conclusions

Herein, EVA/POE/SEBS foams were successfully prepared by SC-N<sub>2</sub> foaming process. The results indicated that the increase of SEBS content led to the decrease of the complex viscosity, elastic modulus and viscosity modulus but the increase of the loss factor. In this case, the cell size and uniformity of the prepared foam increased with the increase of SEBS content, and the density of the foam decreased. When the SEBS content was 20 phr, the density of foam decreased from 0.19 to 0.13 g/cm<sup>3</sup>, which was of great significance for the lightweight of foam. In terms of physical and mechanical properties, the increase of SEBS content led to the decrease in tensile strength, tear strength and hardness of the foam, and the increase of elongation at break, compression permanent deformation and recovery rate. When the SEBS content was 20 phr, the resilience of foam increased from 56 to 61%. However, after 100 000 times of dynamic

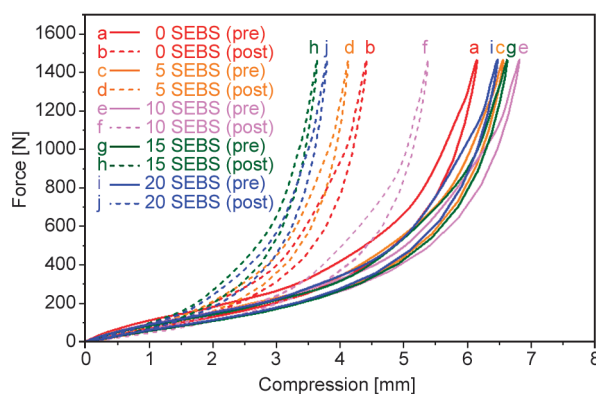


**Figure 7.** Force-compression curve of the foam for pre and post cyclic compression.



compression, the increase of SEBS content led to a gradual decrease in the  $EA/Vol.$  of the foam, while the DCS and stiffness of the foam increased, which was significantly different from the traditional physical and mechanical properties test results and was rarely reported. Therefore, this study provides a new idea for adjusting foam formulation proportion according to actual application scenarios, which is of great significance for practical application.

## References

- [1] Kausar A.: Advances in polymer-anchored carbon nanotube foam: A review. *Polymer-Plastics Technology and Materials*, **58**, 1965–1978 (2019).  
<https://doi.org/10.1080/25740881.2019.1599945>
- [2] Li P., Zhu X., Kong M., Lv Y., Huang Y., Yang Q., Li G.: Fully biodegradable polylactide foams with ultra-high expansion ratio and heat resistance for green packaging. *International Journal of Biological Macromolecules*, **183**, 222–234 (2021).  
<https://doi.org/10.1016/j.ijbiomac.2021.04.146>
- [3] Dai R., Chandrasekaran G., Chen J., Jackson C., Liu Y. M., Nian Q., Kwon B.: Thermal conductivity of metal coated polymer foam: Integrated experimental and modeling study. *International Journal of Thermal Sciences*, **169**, 107045 (2021).  
<https://doi.org/10.1016/j.ijthermalsci.2021.107045>
- [4] Subramonian S., Filiccia P., Alcott J.: Novel soft touch, low abrasion, fine cell polyolefin foams. *Journal of Cellular Plastics*, **43**, 331–343 (2007).  
<https://doi.org/10.1177/0021955X07079070>
- [5] Maiti M., Jasra R. V., Kusum S. K., Chaki T. K.: Microcellular foam from ethylene vinyl acetate/polybutadiene rubber (EVA/BR) based thermoplastic elastomers for footwear applications. *Industrial and Engineering Chemistry Research*, **51**, 10607–10612 (2012).  
<https://doi.org/10.1021/ie300396m>
- [6] Zhang B. S., Lv X. F., Zhang Z. X., Liu Y., Kim J. K., Xin Z. X.: Effect of carbon black content on microcellular structure and physical properties of chlorinated polyethylene rubber foams. *Materials and Design*, **31**, 3106–3110 (2010).  
<https://doi.org/10.1016/j.matdes.2009.12.041>
- [7] Najib N. N., Ariff Z. M., Bakar A. A., Sipaut C. S.: Correlation between the acoustic and dynamic mechanical properties of natural rubber foam: Effect of foaming temperature. *Materials and Design*, **32**, 505–511 (2011).  
<https://doi.org/10.1016/j.matdes.2010.08.030>
- [8] Yang F., Sun H., Mao Z., Tao Y., Zhang J.: Facile fabrication of EVA cellular material with hydrophobic surface, high solar reflectance and low thermal conductivity via chemical foaming. *Microporous and Mesoporous Materials*, **328**, 111460 (2021).  
<https://doi.org/10.1016/j.micromeso.2021.111460>
- [9] Zhang Z. X., Wang Y. M., Zhao Y., Zhang X., Phule A. D.: A new TPE-based foam material from EPDM/PPB blends, as a potential buffer energy-absorbing material. *Express Polymer Letters*, **15**, 89–103 (2021).  
<https://doi.org/10.3144/expresspolymlett.2021.10>
- [10] Fu L., Shi Q., Ji Y., Wang G., Zhang X., Chen J., Shen C., Park C. B.: Improved cell nucleating effect of partially melted crystal structure to enhance the microcellular foaming and impact properties of isotactic polypropylene. *The Journal of Supercritical Fluids*, **160**, 104794 (2020).  
<https://doi.org/10.1016/j.supflu.2020.104794>
- [11] Le Moigne N., Sauceau M., Benyakhlef M., Jemai R., Benezet J.-C., Rodier E., Lopez-Cuesta J.-M., Fages J.: Foaming of poly(3-hydroxybutyrate-co-3-hydroxyvalerate) organo-clays nano-biocomposites by a continuous supercritical CO<sub>2</sub> assisted extrusion process. *European Polymer Journal*, **61**, 157–171 (2014).  
<https://doi.org/10.1016/j.eurpolymj.2014.10.008>
- [12] Sun J., Xu J., He Z., Ren H., Wang Y., Zhang L., Bao J.-B.: Role of nano silica in supercritical CO<sub>2</sub> foaming of thermoplastic poly(vinyl alcohol) and its effect on cell structure and mechanical properties. *European Polymer Journal*, **105**, 491–499 (2018).  
<https://doi.org/10.1016/j.eurpolymj.2018.06.009>
- [13] Sun X., Turng L.-S.: Novel injection molding foaming approaches using gas-laden pellets with N<sub>2</sub>, CO<sub>2</sub>, and N<sub>2</sub> + CO<sub>2</sub> as the blowing agents. *Polymer Engineering Science*, **54**, 899–913 (2014).  
<https://doi.org/10.1002/pen.23630>
- [14] Sato Y., Fujiwara K., Takikawa T., Takishima S., Masuoka H.: Solubilities and diffusion coefficients of carbon dioxide and nitrogen in polypropylene, high-density polyethylene, and polystyrene under high pressures and temperatures. *Fluid Phase Equilibria*, **162**, 261–276 (1999).  
[https://doi.org/10.1016/S0378-3812\(99\)00217-4](https://doi.org/10.1016/S0378-3812(99)00217-4)
- [15] Li G., Gunkel F., Wang J., Park C. B., Altstädt V.: Solubility measurements of N<sub>2</sub> and CO<sub>2</sub> in polypropylene and ethene/octene copolymer. *Journal of Applied Polymer Science*, **103**, 2945–2953 (2007).  
<https://doi.org/10.1002/app.25163>
- [16] Michaeli W., Westermann K., Sitz S.: Extrusion of physically foamed rubber profiles. *Journal of Cellular Plastics*, **47**, 483–495 (2011).  
<https://doi.org/10.1177/0021955X11411251>
- [17] Zhong W. P., Yu Z., Zhu T., Zhao Y., Phule A. D., Zhang Z. X.: Influence of different ratio of CO<sub>2</sub>/N<sub>2</sub> and foaming additives on supercritical foaming of expanded thermoplastic polyurethane. *Express Polymer Letters*, **16**, 318–336 (2022).  
<https://doi.org/10.3144/expresspolymlett.2022.24>
- [18] Pavia Junior C. Z., Peruchi R. S., Fim F. C., de Oliveira Silva Soares W., da Silva L. B.: Performance of ethylene vinyl acetate waste (EVA-w) when incorporated into expanded EVA foam for footwear. *Journal of Cleaner Production*, **317**, 128352 (2021).  
<https://doi.org/10.1016/j.jclepro.2021.128352>



- [19] Zhang Z. X., Dai X. R., Zou L., Wen S. B., Sinha T. K., Li H.: A developed, eco-friendly, and flexible thermoplastic elastomeric foam from SEBS for footwear application. *Express Polymer Letters*, **13**, 948–958 (2019).  
<https://doi.org/10.3144/expresspolymlett.2019.83>
- [20] Ray I., Khastgir D.: Correlation between morphology with dynamic mechanical, thermal, physicomechanical properties and electrical conductivity for EVA-LDPE blends. *Polymer*, **34**, 2030–2037 (1993).  
[https://doi.org/10.1016/0032-3861\(93\)90727-R](https://doi.org/10.1016/0032-3861(93)90727-R)
- [21] Li Y., Gong P., Liu Y., Niu Y., Park C. B., Li G.: Environmentally friendly and zero-formamide EVA/LDPE microcellular foams *via* supercritical carbon dioxide solid foaming. *ACS Applied Polymer Materials*, **3**, 4213–4222 (2021).  
<https://doi.org/10.1021/acsapm.1c00640>
- [22] Sasikala A., Kala A.: Thermal stability and mechanical strength analysis of EVA and blend of EVA with natural rubber. *Materials Today: Proceedings*, **5**, 8862–8867 (2018).  
<https://doi.org/10.1016/j.matpr.2017.12.318>
- [23] Kwon M. J., Lim D. H., Choi I. C., Kwon H-W., Ha C-S.: Preparation and properties of ethylene-vinyl acetate copolymer-based blend foams. *Journal of Elastomers and Plastics*, **53**, 68–82 (2020).  
<https://doi.org/10.1177/0095244319900375>
- [24] Zhang Z. X., Zhang T., Wang D., Zhang X., Xin Z., Prakashan K.: Physicomechanical, friction, and abrasion properties of EVA/PU blend foams foamed by supercritical nitrogen. *Polymer Engineering Science*, **58**, 673–682 (2017).  
<https://doi.org/10.1002/pen.24598>
- [25] Calisi N., Giuliani A., Alderighi M., Schnorr J. M., Swager T. M., Di Francesco F., Pucci A.: Factors affecting the dispersion of MWCNTs in electrically conducting SEBS nanocomposites. *European Journal of Polymers*, **49**, 1471–1478 (2013).  
<https://doi.org/10.1016/j.eurpolymj.2013.03.029>
- [26] Li X., Tang S., Zhou X., Gu S., Huang K., Xu J., Wang X., Li Y.: Synergistic effect of amino silane functional montmorillonite on intumescent flame-retarded SEBS and its mechanism. *Journal of Applied Polymer Science*, **134**, 44953 (2017).  
<https://doi.org/10.1002/APP.44953>
- [27] Li X., Yang J., Zhou X., Wei Q., Li J., Qiu B., Wunderlich K., Wang X.: Effect of compatibilizer on morphology, rheology and properties of SEBS/clay nanocomposites. *Polymer Testing*, **67**, 435–440 (2018).  
<https://doi.org/10.1016/j.polymertesting.2018.03.037>
- [28] Yamaguchi T., Pathomchat P., Shibata K., Nishi T., Tateishi J., Hokkirigawa K.: Effects of porosity and SEBS fraction on dry sliding friction of EVA foams for sports shoe sole applications. *Tribology Transactions*, **63**, 1067–1075 (2020).  
<https://doi.org/10.1080/10402004.2020.1789797>
- [29] Wisinger C. E., Maynarda L. A., Barone J. R.: Bending, curling, and twisting in polymeric bilayers. *Soft Matter*, **15**, 4541–4547 (2019).  
<https://doi.org/10.1039/C9SM00268e>
- [30] Banerjee R., Sinha Ray. S., Ghosh A. K.: Dynamic rheology and foaming behaviour of styrene–ethylene–butylene–styrene/polystyrene blends. *Journal of Cellular Plastics*, **53**, 389–406 (2016).  
<https://doi.org/10.1177/0021955x16652108>
- [31] Pang Y., Wang S., Wu M., Liu W., Wu F., Lee P. C., Zheng W.: Kinetics study of oil sorption with open-cell polypropylene/polyolefin elastomer blend foams prepared via continuous extrusion foaming. *Polymer for Advanced Technology*, **29**, 1313–1321 (2018).  
<https://doi.org/10.1002/pat.4243>
- [32] Wen S., Xin Z., Phule A. D., Zhang Z. X.: Microcellular ethylene-vinyl acetate copolymer foam: Life prediction under reciprocating compression. *Advanced Engineering Materials*, **24**, 2101089 (2022).  
<https://doi.org/10.1002/adem.202101089>
- [33] Yang Z., Liu T., Hu D., Xu Z., Zhao L.: Foaming window for preparation of microcellular rigid polyurethanes using supercritical carbon dioxide as blowing agent. *The Journal of Supercritical Fluids*, **147**, 254–262 (2019).  
<https://doi.org/10.1016/j.supflu.2018.11.001>
- [34] Zhu J., Li X., Weng Y., Tan B., Zhang S.: Fabrication of microcellular epoxidized natural rubber foam with superior ductility by designable chemical and physical crosslinking networks. *The Journal of Supercritical Fluids*, **181**, 105508 (2022).  
<https://doi.org/10.1016/j.supflu.2021.105508>